CHEMISTRY
A European Journal

A Journal of
ChemPubSoc Europe

Accepted Article

Title: A Unique (3+2) Annulation Reaction between Meldrum's Acid and Nitrones: Mechanistic Insight by ESI-IMS-MS and DFT Studies

Authors: Nicolas Lespes, Etienne Pair, Clisy Maganga, Marie Bretier, Vincent Tognetti, Laurent Joubert, Vincent Levacher, Marie Hubert-Roux, Carlos Afonso, Corinne Loutelier-Bourhis, and Jean-François Brière

To be cited as: *Chem. Eur. J.* 10.1002/chem.201705714

Link to VoR: http://dx.doi.org/10.1002/chem.201705714

Supported by
ACES

WILEY-VCH

10.1002/chem.201705714

WILEY-VCH

A Unique (3+2) Annulation Reaction between Meldrum's Acid and Nitrones: Mechanistic Insight by ESI-IMS-MS and DFT Studies

Nicolas Lespes,[a] Etienne Pair,[a] Clisy Maganga,[a] Marie Bretier,[a] Vincent Tognetti,*[a] Laurent Joubert,[a] Vincent Levacher,[a] Marie Hubert-Roux,[a] Carlos Afonso,[a] Corinne Loutelier-Bourhis,*[a] Jean-François Brière*[a]

Dedication ((optional))

Abstract: The fragile intermediates of the domino process leading to isoxazolidin-5-one, triggered by the unique reactivity between Meldrum's acid and *N*-Bn nitrone in the presence of a Brønsted base, were determined thanks to the softness and accuracy of electrospray ionization mass spectrometry coupled to ion mobility spectrometry (ESI-IMS-MS). The combined DFT study shed light on the overall organocatalytic sequence, which starts by a stepwise (3+2) annulation reaction followed by a decarboxylative protonation sequence encompassing a stereoselective pathway issue.

Introduction

1,3-dipolar cycloaddition reactions have become an essential part of organic chemists' portfolio for the construction of ubiquitous five-membered ring heterocycles.[1] Since the seminal investigations of Huisgen and colleagues,[2] a great deal of research has been carried out, not only to extend the scope of these useful annulation processes, but also to ascertain the exact mechanism in action based on either concerted or non-concerted events. We recently reported a unique dipolarophile-like behavior of Meldrum's acid **1** in the presence of nitrone dipoles **2** allowing a straightforward synthesis of isoxazolidin-5-ones **3** (Scheme 1),[3] which are useful building blocks for the elaboration of medicinally relevant β-amino acids or nucleoside mimics.[4] This novel methodology has highlighted (1) the practical use of Meldrum's acid derivatives **1** as a ketene equivalent or C2 synthon;[5] (2) a facile addition reaction of rather acidic Meldrum's acid derivatives **1** (pK_a = 4.93 in water for R^1 = H) to nitrone **2** upon organocatalytic Brønsted base (**R_3N**) conditions despite the poor nucleophilic nature of the anion intermediate **4** (step **I**);[6, 5c] and (3) a domino reaction encompassing likely a formal (3+2) annulation-fragmentation-decarboxylation-protonation sequence towards the formation of product **3** (steps **I**-**III**). Nevertheless, the veracity of these assumptions still has to be addressed in order to shed light on the overall organocatalytic sequence; a requisite endeavor to broaden the scope of this useful organocatalytic process and tackle, eventually, an efficacious asymmetric version.[3a]

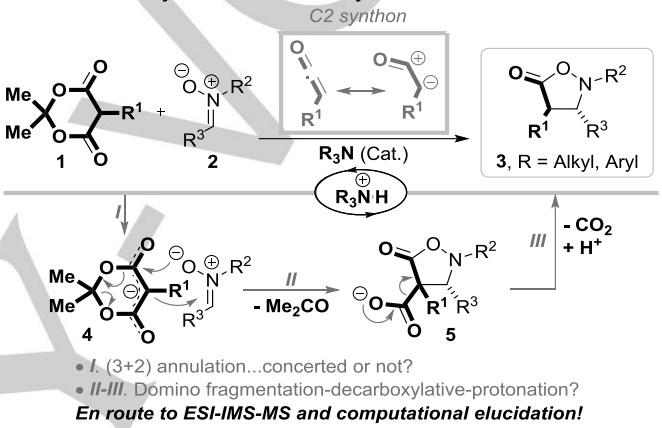

Scheme 1. Organocatalytic Synthesis of Isoxazolidinones and Mechanistic hypotheses to be addressed.

Electrospray ionization mass spectrometry (ESI-MS) along with direct infusion of liquid solutions, proved to be a useful tool that allows the "off-line" monitoring of reactions in almost a real-time mode. The softness of ESI permits the "fishing" of charged and labile synthetic intermediates.[7],[8] This is a salient feature to tackle the determination of heat sensitive species such as the ones putatively encounter from Meldrum's acid **1** (*i.e.* **4** and **5**). Recently, the coupling of ion mobility spectrometry (IMS) technique with MS not only afforded a new dimension for the separation of closely related structures within challenging complex mixtures,[9],[10],[11] but provided novel opportunities for the determination of three-dimensional structures.[12] In IMS, ions are separated as a function of their charge, shape and size through their collision cross-section (CCS, Ω). Experimental CCS values can be determined and compared to those calculated from theoretical structures. Then, ESI-IMS-MS coupled with quantum chemical calculations emerges as a powerful modern strategy to get insights into complex reaction pathways,[13] although its application to mechanistic elucidation endeavors of organocatalytic processes remains underexploited.[7],[10],[14]

We are pleased to report a mechanistic investigation of the (3+2) annulation reaction between Meldrum's acid **1a** (R^1 = H) and a *N*-Bn nitrone **2a** (R^2 = Bn and R^3 = Ph) allowing an unprecedented insight into this useful albeit complex organocatalyzed domino process thanks to the powerfulness of

[a] Dr. N. Lespes,[+] Dr. E. Pair,[+] C. Maganga, M. Bretier, Dr. V. Tognetti, Prof. L. Joubert, Dr. V. Levacher, Dr. M. Hubert-Roux, Prof. C. Afonso, Dr. C. Loutelier-Bourhis, Dr. J.-F. Brière
Normandie Univ, INSA Rouen, UNIROUEN, CNRS, COBRA, 76000 Rouen, France
E-mail: corinne.loutelier@univ-rouen.fr
jean-francois.briere@insa-rouen.fr
vincent.tognetti@univ-rouen.fr
[+] *These authors contributed equally to this work.*

Supporting information for this article is given via a link at the end of the document.((Please delete this text if not appropriate))

the combined real-time reaction monitoring by ESI-IMS-MS and DFT computational study.

Results and Discussion

Preliminary results

The specific reactivity of Meldrum's acid **1a** with *N*-benzyl nitrone dipole **2a** is depicted in Table 1. In the presence of 20 mol% of Hünig base at 40 °C in toluene, a conversion of 68% into isoxazolidinone **3a** was measured by ^{1}H NMR after 2 hours of reaction (entry 1).[3a] Actually, the reaction was completed within 18 hours to give product **3a** in 86% isolated yield (entry 2). The reaction can proceed in other solvents but the faster rate was observed in toluene (entry 2).[3a] On the contrary, hardly no formation of product **3a** was observed in the absence of Brønsted base promoter after 18 hours (entry 3). However, 48% of nitrone **2a** was consumed as estimated by ^{1}H NMR of the crude mixture (see supporting information).

Table 1. Preliminary Investigations.[a]

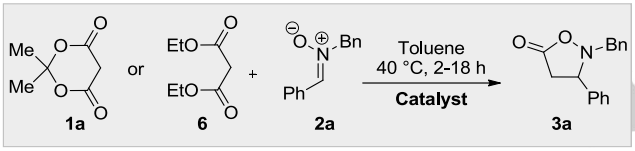

Entry	Precursor	Catalyst (equiv), time	**3a** (%)[b]
1	**1a**	*i*Pr$_2$EtN (0.2), 2 h	68 (64)[c]
2	**1a**	*i*Pr$_2$EtN (0.2), 18 h	(86)[c] (35)[d]
3	**1a**	(0), 18 h	(-)
4	**6**	*i*Pr$_2$EtN (0.2), 2 h	0
5	**6**	TBD (0.2), 2 h	0
6	**1a**	*n*Bu$_4$NBr (0.2), K$_2$CO$_3$ (1), 2 h	32[e]

[a] Meldrum's acid **1a** or diethylmalonate **6** (1.1 equiv), *N*-benzylnitrone **2a** (1 equiv), Catalyst (0.2 equiv), toluene (0.1 M), 2 or 18 hours. [b] Conversion determined by ^{1}H NMR of the crude product with respect to the remaining nitrone **2a**. [c] Isolated yield after silica gel column chromatography. [d] Performed in acetonitrile as solvent. [e] 20% of conversion without *n*Bu$_4$NBr. TBD: triazabicyclo[4.4.0]dec-5-ene.

Despite the help of Hünig base (entry 4) or the strongly basic TBD guanidine (entry 5), the more nucleophilic anion of diethylmalonate **6** did not react with nitrone **2a** and starting materials were recovered. Interestingly, the reaction turned out to be sluggish and not clean upon Phase Transfer Catalysis (PTC) conditions, which may involve a quaternary ammonium (**R$_4$N$^+$**) ion-pair with the anion **4a** of Meldrum's acid **1a** (entry 6). Obviously, a tertiary ammonium salt (**R$_3$N$^+$-H**) flanked to the Meldrum's acid anion **4a** might be the catalytically effective species with (1) an important role of the cation likely as hydrogen bonding donor species and (2) no correlation to the nucleophilic character of the 1,3-dienone type nucleophile.

At the onset of the mechanistic investigation, we attempted to follow the reaction in the presence of Hünig base (20 mol%) in an NMR tube with toluene-d_8 as solvent. It turned out that no intermediate was detected at 40°C demonstrating a rapid process in action. Nevertheless, a major intermediate was observed at 20°C with a relative proportion of 10%, with respect to nitrone **2a** and product **3a** (see supporting information). Despite a much slower process at 20°C the isoxazolidinone **3a** accumulated with up to 78% NMR yield after 24 hours. Then, the reaction conditions for the ESI-MS investigation were set.

Mechanistic investigation by ESI-MS/MS

The first step was the analysis of individual chemical species, namely reagents **1a**, *i*Pr$_2$EtN and **2a** together with the final product **3a**, by ESI-MS (Scheme 2a-b).

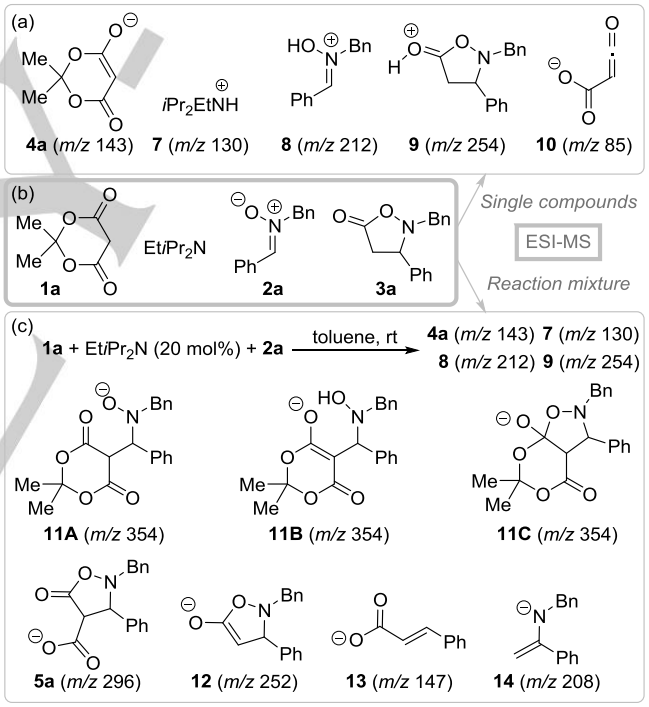

Scheme 2. Proposed structures of ions detected by ESI-MS.

The Hünig base gave an abundant signal corresponding to the ammonium ion 7" instead of ammonium ion **7** signal while protonated nitrone **8** and isoxazolidinone **9** were low-abundant species in the positive ion mode. When the final product was analyzed in the negative ion mode, the deprotonated isoxazolidinone **3a** (ion **12** in Scheme 2c) was not detected, even in the presence of the Hünig base (20 mol%). The deprotonated Meldrum's acid **4a** could be detected in the negative ion mode although some precautions were required. Indeed, the detection of the resulting enolate (*m/z* 143)

necessitates soft source conditions in order to prevent any fragmentation (see supporting information). Accordingly, the increase of either source cone voltage or source temperature induced the known enolate fragmentation with acetone neutral loss leading to *m/z* 85, the acyl-ketene species **10**. This is a well-known reactivity pathway of Meldrum's acid **1a** which has to be taken into account in our investigation.[15]

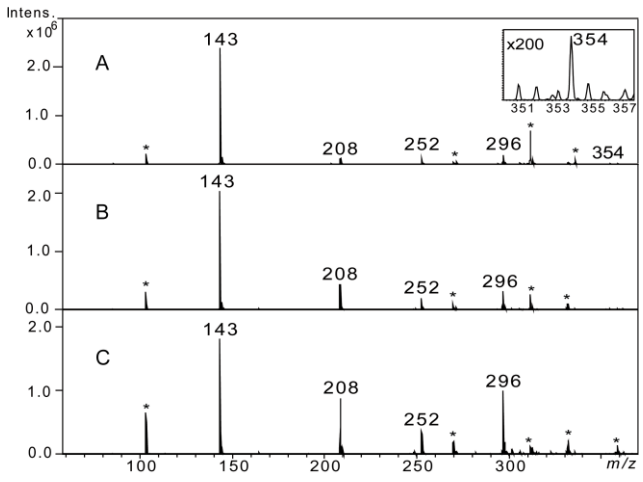

Figure 1. Negative ion ESI mass spectra after 10 min (A), 45 min (B) and 90 min (C) of reaction recorded on the QIT instrument. *Contaminant. Inset show a zoom of *m/z* 350-357 range

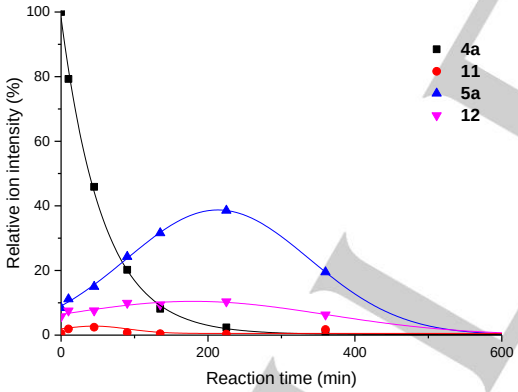

Figure 2. Evolution with time of ion relative intensity of **4a, 5a, 11** and **12** from the ESI-QIT analysis.

Next, the reaction monitoring was carried out in the presence of Hünig base as catalyst (Scheme 2c, Figure 1). The obtained diluted reaction mixtures were thus analyzed at various time intervals (10 minutes, 45 minutes, 1h30, 2h15, 3h45, 6h and 21h) in both negative and positive ion modes. The positive ESI mass spectra only showed the ammonium ion iPr_2EtNH^+ **7** together with the protonated nitrone **8** and isoxazolidinone **9** whereby their abundances increased along the reaction time (data not shown). In the negative ion mode, the anionic intermediates **11** (*m/z* 354), **5a** (*m/z* 296) and **12** (*m/z* 252) appeared as early as 10 minutes, increased with time in a first stage and then decreased. This evolution was confirmed by replicate and a semi-quantitative monitoring of the reaction by infusion of the reaction media at various time intervals in a flow-injection approach using heptadecanoic acid as an internal standard (Figure 2). The relative abundances of **12** and especially carboxylate **5a** followed a Gaussian curve. Meanwhile, the enolate **4a**, the first intermediate in our mechanistic proposal, steadily decreased. The ionic intermediate **11**, hypothesized as one out of three possible isomers **11A-C** at that stage, was a low-abundance species along the reaction but was clearly identified by high-resolution mass spectrometry (*vide infra*). Thanks to the softness of ESI-MS no fragmentation of **4a** into the acyl ketene product **10** was detected ruling out a ketene based mechanism.[16]

To pursue the structural identification of **12**, **11** and **5a** intermediates, tandem mass spectrometry (MS/MS) experiments using collision induced dissociation (CID) activation process were carried out (Figure 3). The product ions observed were comfortingly consistent with the supposed structures. Indeed, the ion at m/z 252 (**12**) dissociates into ions either at m/z 208 (14) or m/z 147 (**13**) which can respectively be explained by elimination of CO_2 or C_7H_7N (Figure 3A). While (**11**) can eliminate one CO_2 molecule, *m/z* 296 dissociates with successive elimination of two CO_2 molecules (leading to *m/z* 252 and *m/z* 208, Figure 3B) which is possible for structure **5a**. Then, *m/z* 354 (**11**) and *m/z* 296 (**5a**) first dissociate into *m/z* 252 and then into some common product ions, *m/z* 208 (**14**) and *m/z* 147 (**13**), which were previously stated for *m/z* 252 (**11**). Common fragmentation patterns indicate that both *m/z* 252 product ions observed in Figure 3B and 3C correspond to structure (**12**). Then, the dissociation of *m/z* 354 (**11**) into *m/z* 252 involves elimination of both CO_2 and C_3H_6O in a concerted manner (Figure 3C) which is possible when fragmentation of a six-membered ring *via* a rearrangement pathway occurs.

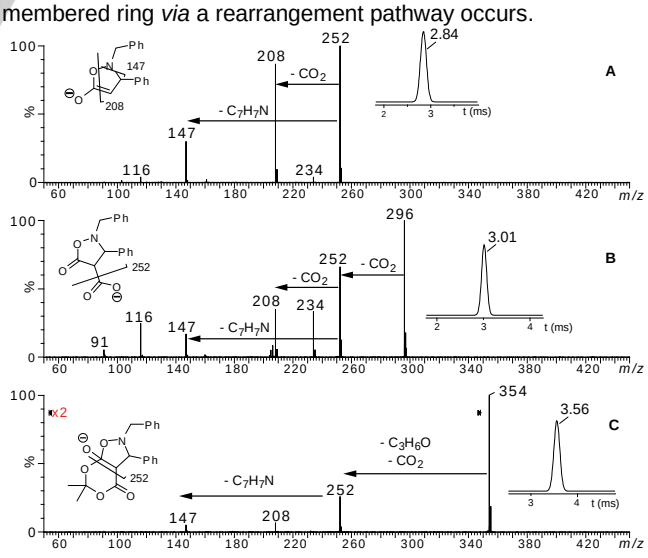

Figure 3. Negative ion ESI-MS/MS spectra of **12** (A), **5a** (B) and **11** (C) precursor ions recorded with the Q-IMS-TOF instrument. The right insets show the ion mobility spectra of the corresponding precursor ions while the left insets display their fragmentation patterns.

It is remarkable that transient and likely enolate species **12** (*m/z* 252) was detected in the reaction media given the expected fast protonation event of this basic last intermediate of the domino sequence (*vide infra*). At that stage, we cannot rule out that part of the *m/z* 252 (**12**) is originated from some fragmentation of *m/z* 296, namely carboxylate **5a**, inside the mass spectrometer.

Eventually, the elemental composition of the detected species from MS and MS/MS experiments was determined by accurate mass measurements using the Q-IMS-TOF mass spectrometer and, pleasingly, matched with the supposed intermediates **4a**, **5a**, **11** and **12** (Table 2).

Table 2. Accurate mass measurements, elemental composition of ions.

Ion (*m/z*)	Experimental (*m/z*)	Calculated (*m/z*)	ΔM (ppm)	Elemental composition	ions
143	143.0341	143.0349	4.9	$C_6H_7O_4$	**4a**
252	252.1021	252.1030	3.6	$C_{16}H_{14}NO_2$	**12**
296	296.0930	296.0928	-0.7	$C_{17}H_{14}NO_4$	**5a**
354	354.1332	354.1347	4.2	$C_{20}H_{20}NO_5$	**11**
147	147.0444	147.0451	4.8	$C_9H_7O_2$	**13**
208	208.1126	208.1132	2.9	$C_{15}H_{14}N$	**14**

Computational study

In line with the ESI-IMS-MS study, density functional theory (DFT) calculations were performed in order to investigate the possible reaction pathways and intermediates for the synthesis of isoxazolidin-5-one **3a** (Scheme 3). The first step consists in the formation of the noncovalent adduct **Int1** between the enolate **4a** and the nitrone **2a**, which displays a hydrogen-bonding interaction with the protonated trimethylamine. This interaction likely enhances the electrophilic character of nitrone **2a** and promotes the subsequent nucleophilic addition reaction of Meldrum acid enolate **4a**. The formation of the C-C bond takes place through transition state **TS1** and the protonation of nitrone **2a**, which occur at the same single step (with an overall activation barrier equal to 14.6 kcal/mol), affording intermediate **Int2**. This compound then undergoes a cyclization by the formation of a C-O bond (see dashed line in **TS2**) associated to a second proton transfer from the hydroxylamine moiety to trimethylamine, along with a moderate activation barrier (11.9 kcal/mol). Interestingly, this ring-opening reaction leads first to an alcoholate intermediate **Int3** showing that the formal fragmentation event occurs in two steps. Accordingly, an acetone molecule can be exothermically eliminated from **Int3** by the relevant C-O bond breaking at a low energetic cost (6.4 kcal/mol), leading to the relatively stable carboxylate intermediate **Int4**. The activation barrier **TS4** (26.0 kcal/mol) for the subsequent decarboxylation reaction providing intermediate **Int5** is markedly higher than those for the nucleophilic addition and cyclization steps (**Int1** to **Int2** to **Int3**).[17] Finally, the rather unstable enolate **Int5** (or **12** in MS) rapidly evolves towards the much more stable isoxazolidin-5-one product **3a**, which is obtained by the C-protonation and regeneration of the amine-catalyst, as described in detail in the supplementary information. These computational results are consistent with the MS study, which showed the accumulation of the carboxylate intermediate **5a** *in situ* (Figure 2). At first glance, the close energy between **TS1** and **TS2**, namely the addition and cyclisation steps of the (3+2) annulation sequence, may account for the modest enantiomeric excesses previously obtained on this system thus far, due to some equilibration events of the first enantio-relevant addition step.[3a]

However, one should not forget that mass spectrometry only analyzes charged species in gas phase (*after desolvation of the ions by ESI from the reaction media diluted in acetonitrile*), whereas the previous reaction pathway was studied in the presence of a protonated trimethylamine counterion in acetonitrile solution, to be close to the experimental conditions of the organic synthesis. While, the release of acetone and decarboxylation were found to be almost unaffected by the presence of the counteranion (see SI for an exhaustive description), the addition and cyclization steps appeared to be strongly influenced by the presence of the protonated trimethylamine either in gas phase or solvent as shown in Scheme 4. Indeed, as revealed by intrinsic reaction coordinate (IRC) calculations in the absence of Me_3N^+H, the initial two stages process (addition and cyclization sequence – previously **Int1** to **Int3** with Me_3N) occur in the same step leading directly to **Int7** (or **Int9** in gas phase), through a concerted (3+2)-cycloaddition.[18] Accordingly, the ion of *m/z* 354 seen by ESI-MS likely refers to cyclic-structure **11C** (see Scheme 2). Besides, the associated activation barrier is considerably higher (more than twice than that for the catalyzed version in solution), proving the fundamental role of the R_3N species to facilitate and influence the first steps of this domino process.

10.1002/chem.201705714

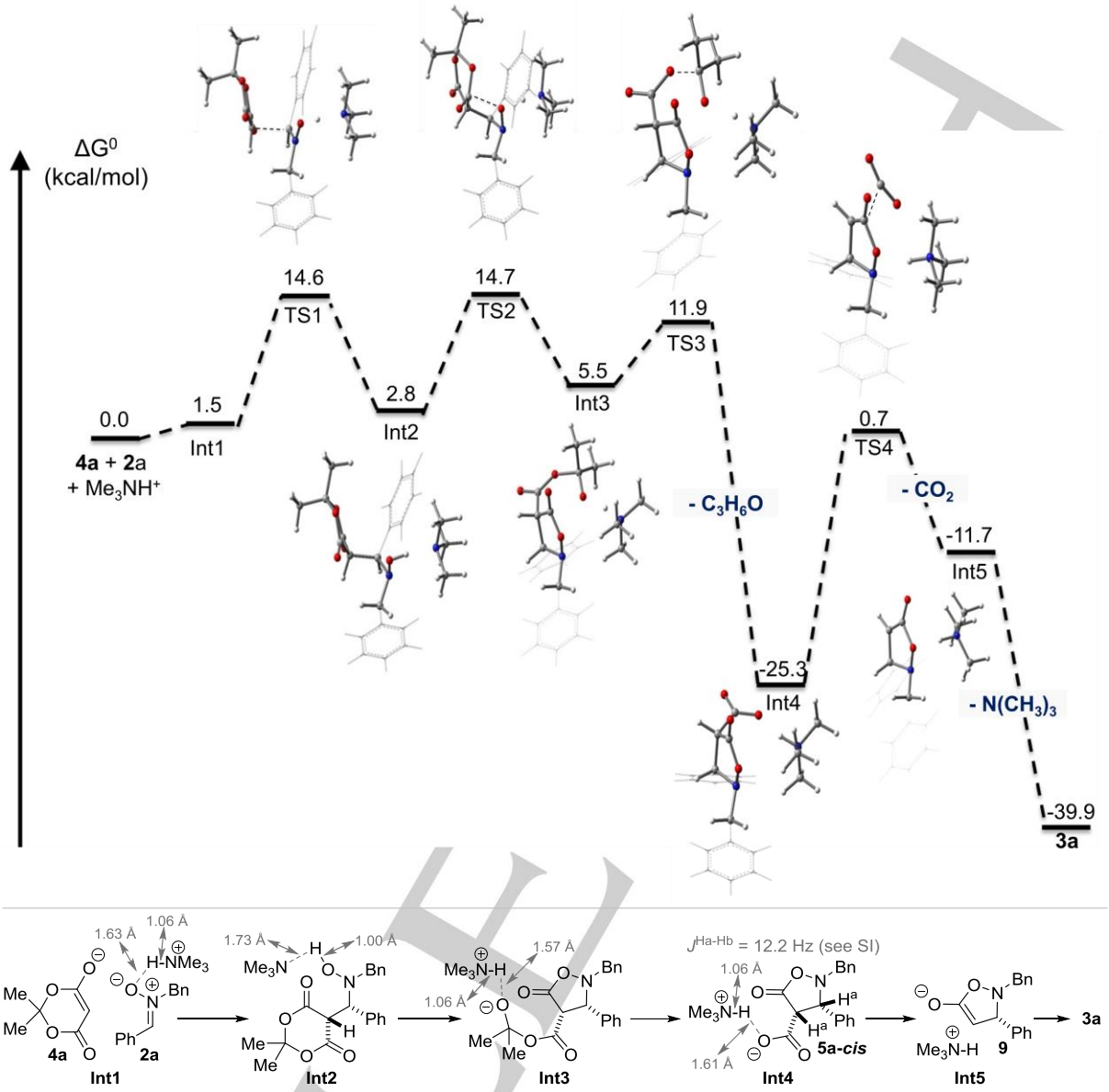

Scheme 3. Standard Gibbs energy profile for the formation of isoxazolidin-5-one **3a** in acetonitrile through the *cis*-carboxylate intermediate **5a-*cis*** (Oxygen atoms in red, nitrogen in blue, carbon in grey, hydrogen in white).

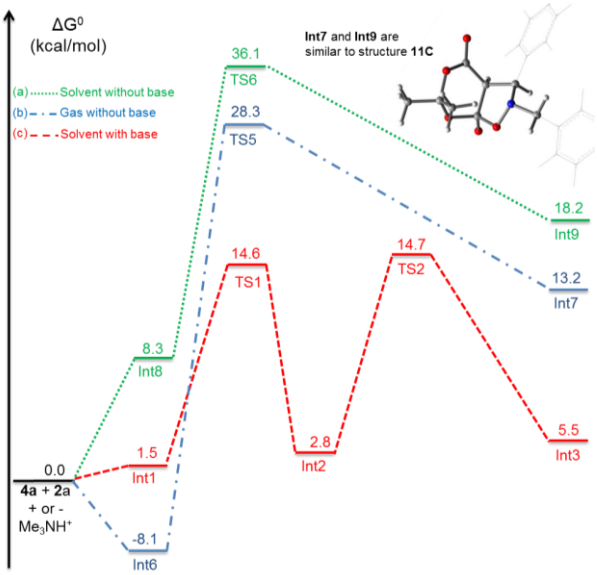

Scheme 4. Standard Gibbs energy profile for the whole cycloaddition process in various environments. (a) In acetonitrile without Me_3N (3D structure displayed is similar to intermediate **11C**). (b) In gas phase process without Me_3N. (c) In acetonitrile with Me_3N as a base catalyst. (Oxygen atoms in red, nitrogen in blue, carbon in grey, hydrogen in white).

One can also investigate stereochemistry issues by the same theoretical protocol (Scheme 5 *versus* Scheme 3). Subsequent to the first addition reaction step, the cyclization event may occur on one of the two diastereotopic carbonyl functional groups of the 2,2-dimethyl-1,3-dioxan-4,6-dione moiety leading to the formation of either *cis* (**Int3**) or *trans*-intermediates (**Int12**). To this aim, the two competing pathways are compared in Scheme 5. Noteworthy, it was found that the two intermediates, **Int2** (*cis* pathway) and **Int11** (*trans* pathway), are energetically close, and can be easily interconverted (the activation barrier being equal to 6 kcal/mol) and are thus in equilibrium. This is no longer the case at the following step, since the Gibbs energies for **Int3** and **Int12** significantly differ. The low stabilization of this last compound strengthens the reversibility of the *trans* path (reverse activation barrier equal to 4.5 kcal/mol). One can notice that intermediate **Int3** (*cis* pathway) resulted from an early ring opening process (C-O bond breaking), on the contrary to the cyclic quaternary alcoholate **Int12** obtained in the *trans* pathway (Scheme 5). That might account why **Int12** is more prone to reverse back to the **Int11**, en route to the *cis* path. Importantly, a major intermediate was seen during a preliminary investigation of this reaction by ^1H NMR reaction which was supposed to be carboxylate **5a** with regard to the ESI-MS kinetic analysis (see Figure 3). The coupling constant of 12.2 Hz (doublet) is related to a *cis* junction of the isoxazolidinone ring of **5a-*cis*** which is consistent with the preferred *cis*-pathway (see Scheme 3).

Mechanistic probe by ESI-IMS-MS and DFT

While collision cross-section (CCS) values can be obtained from DFT optimized structures, used as input in the open source software program MOBCAL,[19],[20] the experimental CCS can be determined from the ESI-IMS-MS data (Table 3). The comparison and the fitting of experimental and calculated CCS values should permit to validate the theoretically determined structures. Among the three different models used to calculate CCS with MOBCAL, the trajectory method (TM), which is considered as the most reliable approach for small organic molecules was used to calculate the CCS values of the intermediates. Meanwhile, the experimental CCS values were determined using the measured drift time of the ions in optimized IMS conditions and the calibration method described in the literature (in He) using dextran oligomer ions as reference ions to correct the non-uniform electric field of the TWIM cell.[21],[22] The CCS values of the intermediates **11C**, **5a** and **12** are reported in Table 3. Pleasingly, these experimental CCS values match with the calculated CCS obtained from the DFT studies which turned out to be the structures of intermediates **5a-cis**, **11C** and **12** (Scheme 2 *versus* Scheme 3).

Table 3. Experimental $^{TW}CCS_{He}$ and calculated CCS of **11C**, **5a** and **12**

	11C	**5a-cis**	**12**
$^{TW}CCS_{He}$ (Å^2)	119 ± 2	107 ± 2	101 ± 2
Calculated CCS (Å^2)	119 ± 6	107 ± 6	99 ± 6

Conclusions

This work highlights the usefulness of the combined ESI-IMS-MS and DFT investigation in order to get insights into complex organocatalytic domino processes involving rather labile intermediates. Upon the direct infusion of a solution of Meldrum's acid **4a**, nitrone **2a** and a Brønsted base, an original sequence leading to isoxazolidinone architecture **3a** was probed for the first time. The soft ESI-MS techniques allowed the "off-line" detection of negatively charged intermediates and IMS-MS permitted the comparison between experimental/theoretical collision cross-section values. With regard to the ESI-MS outcome, the DFT study revealed a sequence triggered by a stepwise (3+2) annulation reaction between Meldrum's acid **4a** and nitrone **2a** favored by the Brønsted base organocatalyst (R_3N) upon hydrogen bonding. The cyclisation steps turned out to occur along a stereoselective pathway giving rise to a *cis*-carboxylate transient species which undergoes a base-promoted decarboxylation (highest energy transition step) followed by a facile protonation sequence. The similarity between the energies of the addition and cyclization steps might explain the low selectivity obtained for the enantioselective version thus far. Based on this knowledge, barely addressed in the chemistry of Meldrum's acid,[13] the scope of this unique cycloaddition-based reactivity with nitrone dipoles is currently under investigation to develop a more broadly applicable methodology and tackle an enantioselective version.

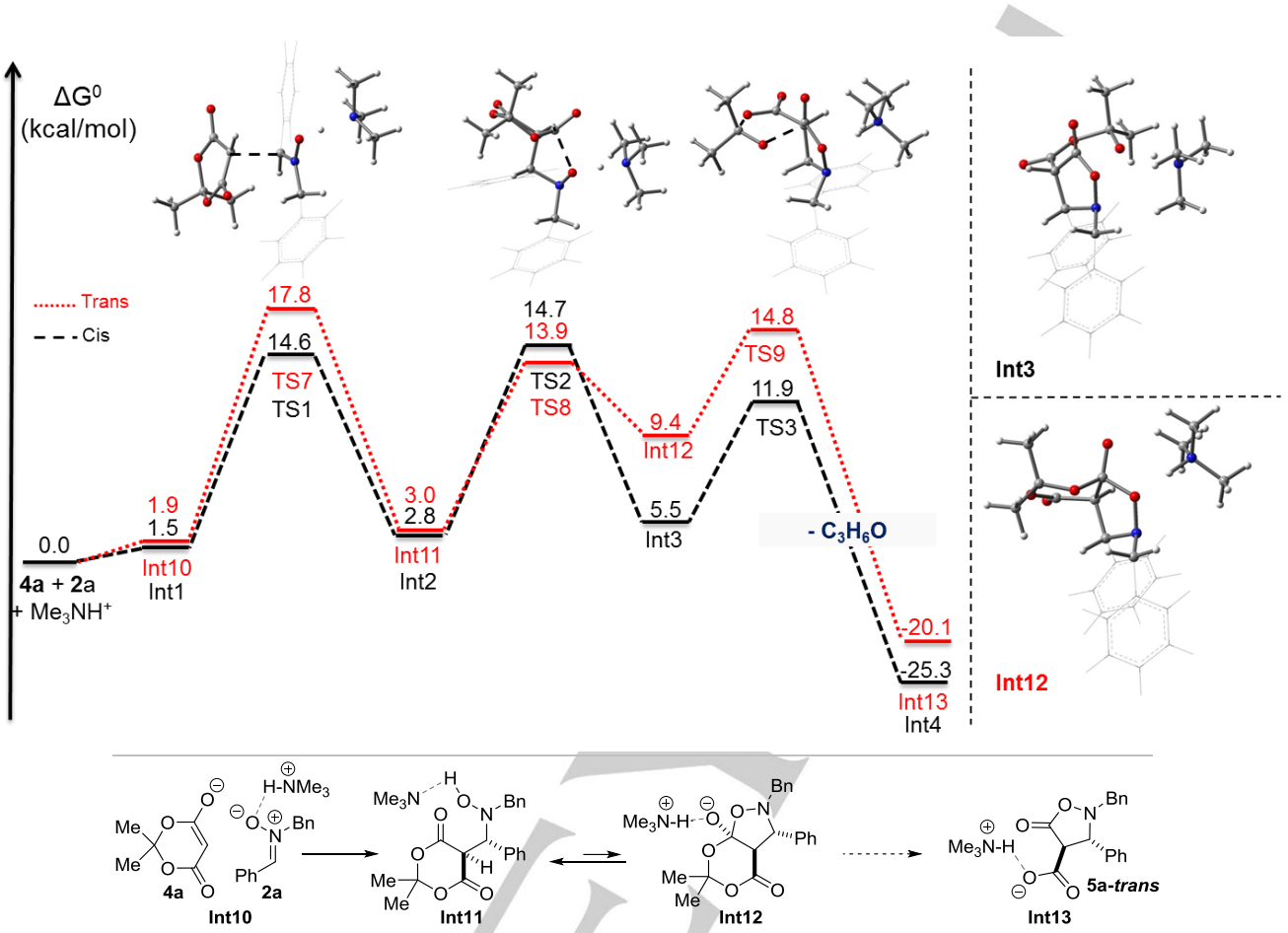

Scheme 5. Standard Gibbs energy profile for the formation of isoxazolidin-5-one **3a** either (a) through the *cis*-carboxylate intermediate **5a-cis** or (d) through *trans*-carboxylate intermediate **5a-trans**. Only transition states of the *trans* pathway are depicted. (Oxygen atoms in red, nitrogen in blue, carbon in grey, hydrogen in white).

Experimental Section

The reaction monitoring was performed by infusing reaction media at different time intervals into the ESI source of the mass spectrometer.

To cross-validate and ensure our results, with regard to the heat sensitivity of transient species, two mass spectrometers were used; (1) a quadrupole ion trap (HCT Ultra ETD II, Bruker) and (2) a quadrupole-ion mobility-time of flight (Synapt G2 HDMS, Waters), both equipped with ESI source. The QIT instrument is equipped with a LC pump-injector system allowing flow-injection analysis (FIA) and was used for semi-quantitative monitoring. The Q-IMS-TOF is equipped with a travelling wave ion mobility (TWIM) cell, previously described,[23] and was used for accurate mass measurements, MS/MS and IMS-MS experiments. MS/MS experiments involved selection of the precursor ion with the quadrupole mass analyzer and CID in the transfer cell using argon as collision gas. Sample solutions were infused into the ESI (Q-IMS-TOF) source using a Cole-Palmer syringe pump. Note that ions of the studied intermediates could be detected at soft source conditions (from 30°C to 50°C desolvation gas temperature) with the ESI source of the QIT instrument to avoid fragmentation of the most fragile species. Some in-source fragmentation was observed with the Q-TOF for the fragile intermediate ion **4a** (see SI).

The TWIM cell is operating with a non-uniform electric field that prevents direct CCS determination. To estimate TWIM CCS, a calibration with reference compounds of known CCS is required.[21] In negative ion mode, various CCS calibrants have been recently described including dextran or fatty acid ions whose CCS have been determined in He or N_2 drift gases.[22],[21d] The extracted ion mobility spectra were fitted using Origin Pro 9.1 software (OriginLab, Northampton, MA, USA).

Computational details

Density Functional Theory (DFT) calculations were carried out with Gaussian 09 program in order to gain insight into the structures of gas phase ions and into the reaction mechanism in a solvent medium.[24] The (dispersion-corrected range-separated hybrid) ωB97X-D exchange-

correlation functional was used in conjunction with the 6-311++G(d,p) triple-ζ basis set for all atoms.[25] Solvent effects were implicitly described by the latest implementation of the IEF polarizable continuum model (IEF-PCM).[26] Vibrational analyses were carried out to determine the nature of the stationary points, and additional intrinsic reaction coordinate (IRC) calculations were run to confirm the connection between reactants and products.[27] The MOBCAL software was used in complement to generate CCS values from these DFT optimized structures using default Lennard-Jones parameters and computed APT atomic charges.[19],[20]

Acknowledgements

This work has been partially supported by INSA Rouen, Rouen University, CNRS, EFRD and Labex SynOrg (ANR-11-LABX-0029) and region Normandie (CRUNCh network). This research was supported by the French National Research Agency (ANR) as part of the ANR-16-CE07-0011-01 project OMaChem.

Keywords: Meldrum's acid • organocatalysis • density functional calculations • mass spectrometry • ion mobility

[1] For recent reviews on dipolar cycloadditions, see: a) T. Hashimoto, K. Maruoka, *Chem. Rev.* **2015**, *115*, 5366; b) M. S. Singh, S. Chowdhury, S. Koley, *Tetrahedron* **2016**, *72*, 1603.

[2] a) R. Huisgen, *Angew. Chem. Int. Ed.* **1963**, *2*, 565; b) R. Huisgen, *Angew. Chem. Int. Ed.* **1963**, *2*, 633.

[3] a) S. Postikova, T. Tite, V. Levacher, J.-F. Brière, *Adv. Synth. Catal.* **2013**, *355*, 2513; b) T. Tite, M. Sabbah, V. Levacher, J.-F. Brière, *Chem. Commun.* **2013**, *49*, 11569.

[4] For reviews on isoxazolidinones and derivatives, see: a) M. Berthet, T. Cheviet, G. Dujardin, I. Parrot, J. Martinez, *Chem. Rev.* **2016**, *116*, 15235; b) J. Annibaletto, S. Oudeyer, V. Levacher, J.-F. Brière, *Synthesis* **2017**, *49*, 2117.

[5] For review on Meldrum's acid, see: a) A. S. Ivanov, *Chem. Soc. Rev.* **2008**, *37*, 789; b) A. M. Dumas, E. Fillion, *Acc. Chem. Res.* **2010**, *43*, 440; c) E. Pair, T. Cadart, V. Levacher, J.-F. Brière, *ChemCatChem* **2016**, *8*, 1882.

[6] Meldrum's acid is 10^6 less reactive than the corresponding ester of malonate: O. Kaumanns, H. Mayr, *J. Org. Chem.* **2008**, *73*, 2738.

[7] a) S. R. Wilson, J. Perez, A. Pasternak, *J. Am. Chem. Soc.* **1993**, *115*, 1994; b) L. S. Santos, *Eur. J. Org. Chem.* **2008**, 235; c) K. L. Vikse, J. S. McIndoe, *Pure Appl. Chem.* **2015**, *87*.

[8] L. S. Santos, C. H. Pavam, W. P. Almeida, F. Coelho, M. N. Eberlin, *Angew. Chem. Int. Ed.* **2004**, *43*, 4330; *Angew. Chem.* **2004**, *116*, 4430.

[9] K. M. Roscioli, X. Zhang, S. X. Li, G. H. Goetz, G. Cheng, Z. Zhang, W. F. Siems, H. H. Hill, *Int. J. Mass Spectrom.* **2013**, *336*, 27.

[10] For a recent investigation of an organocatalytic reaction by ESI-IM-MS, see: J.-T. Zhang, H.-Y. Wang, X. Zhang, F. Zhang, Y.-L. Guo, *Catal. Sci. Technol.* **2016**, *6*, 6637.

[11] a) A. Revesz, D. Schroder, T. A. Rokob, M. Havlik, B. Dolensky, *Angew. Chem. Int. Ed.* **2011**, *50*, 2401; *Angew. Chem*. **2011**, *123*, 2449; b) V. Domalain, V. Tognetti, M. Hubert-Roux, C. M. Lange, L. Joubert, J. Baudoux, J. Rouden, C. Afonso, *J. Am. Soc. Mass Spectrom.* **2013**, *24*, 1437; c) . C. Lapthorn, F. Pullen, B. Z. Chowdhry, *Mass Spectrom. Rev.* **2013**, *32*, 43.

[12] V. D'Atri, M. Porrini, F. Rosu, V. Gabelica, *J. Mass Spectrum.* **2015**, *50*, 711.

[13] Few DFT studies have addressed the understanding of the Meldrum's acid chemical transformation especially the fragmentation event; see reprensative examples: a) S. Perreault, M. Poirier, P. Léveillé, O. René, P. Joly, Y. Dory, C. Spino, *J. Org. Chem.* **2008**, *73*, 7457; b) Representative DFT studies to Meldrum's acid based reactions, see: F. A. Leibfarth, M. Wolffs, L. M. Campos, K. Delany, N. Treat, M. J. Kade, B. Moon, C. J. Hawker, *Chem. Sci.* **2012**, *3*, 766.

[14] For a representative example of IM-MS/DFT Study getting insight into organometallic mechanism, see: G.-J. Cheng, P. Chen, T.-Y. Sun, X. Zhang, J.-Q. Yu, Y.-D. Wu, *Chem.-Eur. J.* **2015**, *21*, 11180.

[15] For a review on acylketenes from Meldrum's acid, see K. P. Reber, S. D. Tilley, E. J. Sorensen, *Chem. Soc. Rev.* **2009**, *38*, 3022.

[16] L. S. Santos, B. A. DaSilveira Neto, C. S. Consorti, C. H. Pavam, W. P. Almeida, F. Coelho, J. Dupont, M. N. Eberlin, *J. Phys. Org. Chem.* **2006**, *19*, 731.

[17] We also computed the activation barrier for this rate-determining step in toluene as solvent. It was found to be slightly lower (24.7 kcal/mol), in agreement with our experimental data.

[18] E. Falkowska, V. Tognetti, L. Joubert, P. Jubault, J.-P. Bouillon, X. Pannecoucke, *RSC Advances* **2015**, *5*, 6864.

[19] A. A. Shvartsburg, M. F. Jarrold, *Chem. Phys. Lett.* **1996**, *261*, 86.

[20] M. F. Mesleh, J. M. Hunter, A. A. Shvartsburg, G. C. Schatz, M. F. Jarrold, *J. Phys. Chem.* **1996**, *100*, 16082.

[21] a) B. T. Ruotolo, J. L. Benesch, A. M. Sandercock, S. J. Hyung, C. V. Robinson, *Nat. Protoc.* **2008**, *3*, 1139; b) D. Smith, T. Knapman, I. Campuzano, R. W Malham, J. Berryman, S. E Radford, A. Ashcroft, *Eur J Mass Spectrom (Chichester, Eng)* **2009**, *15*, 113; c) M. F. Bush, I. D. Campuzano, C. V. Robinson, *Anal. Chem.* **2012**, *84*, 7124; d) J. G. Forsythe, A. S. Petrov, C. A. Walker, S. J. Allen, J. S. Pellissier, M. F. Bush, N. Hud, F. Fernandez, *Analyst* **2015**, 6853.

[22] a) J. Hofmann, W. B. Struwe, C. A. Scarff, J. H. Scrivens, D. J. Harvey, K. Pagel, *Anal. Chem.* **2014**, *86*, 10789; b) F. Zhang, S. Guo, M. Zhang, Z. Zhang, Y. Guo, *J. Mass Spectrum.* **2015**, *50*, 906.

[23] a) K. Giles, S. D. Pringle, K. R. Worthington, D. Little, J. L. Wildgoose, R. H. Bateman, *Rapid Commun. Mass Spectrom.* **2004**, *18*, 2401; b) K. Giles, J. P. Williams, I. Campuzano, *Rapid Commun. Mass Spectrom.* **2011**, *25*, 1559.

[24] M.J. Frisch, G.W. Trucks, H.B. Schlegel, G.E. Scuseria, M.A. Robb, J.R. Cheeseman, G. Scalmani, V. Barone, B. Mennucci, G.A. Petersson, H. Nakatsuji, M. Caricato, X. Li, H.P. Hratchian, A.F. Izmaylov, J. Bloino, G. Zheng, J.L. Sonnenberg, M. Hada, M. Ehara, K. Toyota, R. Fukuda, J. Hasegawa, M. Ishida, T. Nakajima, Y. Honda, O. Kitao, H. Nakai, T. Vreven, J.A. Montgomery Jr., J.E. Peralta, F. Ogliaro, M.J. Bearpark, J. Heyd, E.N. Brothers, K.N. Kudin, V.N. Staroverov, R. Kobayashi, J. Normand, K. Raghavachari, A.P. Rendell, J.C. Burant, S.S. Iyengar, J. Tomasi, M. Cossi, N. Rega, N.J. Millam, M. Klene, J.E. Knox, J.B. Cross, V. Bakken, C. Adamo, J. Jaramillo, R. Gomperts, R.E. Stratmann, O. Yazyev, A.J. Austin, R. Cammi, C. Pomelli, J.W. Ochterski, R.L. Martin, K. Morokuma, V.G. Zakrzewski, G.A. Voth, P. Salvador, J.J. Dannenberg, S. Dapprich, A.D. Daniels, Ö. Farkas, J.B. Foresman, J.V. Ortiz, J. Cioslowski, D.J. Fox. Gaussian 09 rev. D01, Gaussian, Inc., Wallingford, CT, USA (2009).

[25] J.-D. Chai, M. Head-Gordon, *Phys. Chem. Chem. Phys.* **2008**, *10*, 6615.

[26] G. Scalmani, M. J. Frisch, *J. Phys. Chem.* **2010**, *132*, 114110.

[27] K. Fukui, *Acc. Chem. Res.* **1981**, *14*, 363.

10.1002/chem.201705714

WILEY-VCH

Entry for the Table of Contents (Please choose one layout)

Layout 2:

FULL PAPER

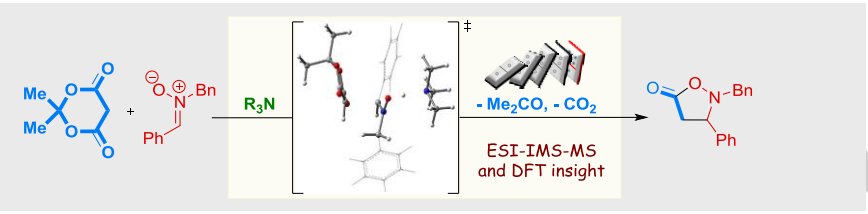

The fragile intermediates of the domino process leading to isoxazolidin-5-one, triggered by the unique reactivity between Meldrum's acid and *N*-Bn nitrone in the presence of a Brønsted base, were determined thanks to the off-line ESI-IMS-MS technic. The combined DFT study shed light on the overall organocatalytic pathway which starts by a stepwise (3+2) annulation reaction followed by a decarboxylative protonation sequence

Nicolas Lespes, Etienne Pair[] Clisy Maganga, Marie Bretier, Vincent Tognetti, Laurent Joubert, Vincent Levacher, Marie Hubert-Roux, Carlos Afonso, Corinne Loutelier-Bourhis,* Jean-François Brière**

Page No. – Page No.

A Unique (3+2) Annulation Reaction between Meldrum's Acid and Nitrones: Mechanistic Insight by ESI-IMS-MS and DFT Studies